

Stereocontrolled Solid-Phase Synthesis of Phosphate/Phosphorothioate (PO/PS) Chimeric Oligodeoxyribonucleotides on an Automated Synthesizer Using an Oxazaphospholidine–Phosphoramidite Method

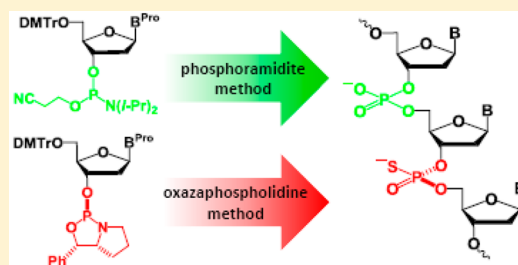
Yohei Nukaga,[†] Natsuhisa Oka,[‡] and Takeshi Wada^{*,†}

[†]Department of Medicinal and Life Sciences, Faculty of Pharmaceutical Sciences, Tokyo University of Science, 2641 Yamazaki, Noda, Chiba 278-8510, Japan

[‡]Department of Chemistry and Biomolecular Science, Faculty of Engineering, Gifu University, 1-1 Yanagido, Gifu 501-1193, Japan

S Supporting Information

ABSTRACT: Stereocontrolled solid-phase synthesis of phosphate/phosphorothioate chimeric oligodeoxyribonucleotides (PO/PS-ODNs) was achieved by integrating the conventional phosphoramidite method into a previously developed oxazaphospholidine method for the stereocontrolled synthesis of *P*-chiral oligonucleotides. *P*-Stereodefined PO/PS-ODNs with mixed sequences (up to 12-mers) were obtained in good yields and high stereoselectivities by reacting different combinations of monomers (conventional phosphoramidites/diastereopure nucleoside 3'-*O*-oxazaphospholidines), activators (ETT/CMPT), capping reagents (Pac₂O/CF₃COIm), and oxidizing/sulfurizing reagents (TBHP/POS) on an automated synthesizer. A thermal denaturation study examined the resultant diastereopure PO/PS-ODN 12-mers with three consecutive (*Rp*)- or (*Sp*)-PS-linkages at the internal or terminal regions of the molecules. We found that (*Rp*)-PO/PS-ODNs can only moderately destabilize duplexes with complementary oligoribonucleotides (ORNs) compared with their unmodified ODN counterparts ($\Delta T_m = -0.4$ °C per modification). In contrast, (*Sp*)-PO/PS-ODNs have larger destabilizing effects ($\Delta T_m = -1.2$ to -0.8 °C per modification). Although smaller destabilizing effects were observed when the (*Sp*)-PS-linkages were incorporated into the terminal regions of the molecule, there was a weaker correlation between the location of an incorporated (*Rp*)-PS-linkage and its destabilizing effect.



INTRODUCTION

In phosphorothioate oligodeoxyribonucleotides (PS-ODNs), a sulfur atom replaces a nonbridging oxygen atom on each phosphodiester linkage of an oligodeoxyribonucleotide (ODN). PS-ODNs are widely used as key structures in therapeutic oligonucleotides because of their enhanced stability in the presence of nucleases, cell-membrane permeability, and favorable pharmacokinetics.¹ However, PS-ODNs with fully modified phosphorothioate backbones suffer from certain therapeutic drawbacks such as cytotoxicity at high concentrations and low affinities for complementary RNAs (in comparison with unmodified ODNs).^{1,2} Phosphate/phosphorothioate chimeric oligodeoxyribonucleotide (PO/PS-ODN) structures have emerged as a promising candidate for therapeutic oligonucleotides because these compounds overcome the deficiencies that are commonly observed in PS-ODNs.^{2,3}

The PS-linkages in PO/PS-ODNs possess a chiral center at each phosphorus atom; certain biological and physicochemical properties such as their affinity for complementary RNAs, stability to nucleases, RNase H activity, and gene silencing potency are potentially dependent on the stereochemical configurations of these phosphorus atoms.^{1d,4–9} It is therefore

critical to develop an efficient method for the synthesis of *P*-stereodefined PO/PS-ODNs. Although PO/PS-ODNs with one stereodefined PS-linkage at a specific position can be effectively isolated by a chromatographic separation of diastereomixtures,⁵ this method is generally inapplicable to the isolation of PO/PS-ODNs with multiple stereodefined PS-linkages. Diastereopure dimer building blocks have previously been used to incorporate multiple stereodefined PS-linkages into ODNs;⁶ however, this method requires up to 32 different types of building blocks and is inapplicable to the preparation of PO/PS-ODNs with consecutive stereodefined PS-linkages. The stereocontrolled synthesis of PO/PS-ODNs with multiple stereodefined PS-linkages at either consecutive or discrete positions has been achieved with the oxathiaphospholane method,^{7,10} which uses nucleoside 3'-*O*-oxathiaphospholane monomers to synthesize both unmodified PO-linkages and stereodefined PS-linkages.^{10c} A recent report has demonstrated that the oxathiaphospholane method can be combined with the conventional phosphoramidite method¹¹ to synthesize *P*-stereodefined PO/PS-ODNs.^{10e} However, the chromatographic

Received: December 13, 2015

Published: March 3, 2016

Table 1. Solid-Phase Synthesis of Unmodified ODN 5-mers 8–11 Using CMPT as the Activator

entry	PO/PS-ODN ^a	Im (M)	coupling yield (%) ^a	
			third	fourth
1	d(TTTT) 8	0	143	173
2	d(CCCCT) 9	0	116	115
3	d(AAAAT) 10	0	117	120
4	d(GGGGT) 11	0	114	110
5	d(TTTT) 8	0.05	128	141
6	d(TTTT) 8	0.1	106	110
7	d(TTTT) 8	0.2	101	99
8	d(TTTT) 8	0.3	99	100

^aDetermined by DMTr⁺ assay.

(e.g., 1*H*-tetrazole). We reasoned that the low nucleophilicity of CMPT enabled the *O*⁴-phosphites in this study to survive.^{16c} To confirm the presence of the *O*⁴-phosphite, we performed ³¹P NMR analysis on the condensation reaction of **1a** with 3'-*O*-DMTr-thymidine **12** in the presence of CMPT (Scheme 2). The spectrum showed minor signals around δ 130 ppm, which were in the same range as the signals of *O*⁶-phosphitylguanines reported in the literature.^{16b} In addition, intense signals around δ 140 ppm corresponded to the phosphite triester, which indicated that *O*⁴-phosphites were present as minor products.¹⁷

To eliminate byproducts, 0.05–0.3 M imidazole was added to the capping reagents. We expected the reagent to behave as a nucleophile and remove the *O*⁴-phosphites.¹⁸ Entries 5–8 in Table 1 show that the *O*⁴-phosphites were completely removed in the presence of 0.2–0.3 M imidazole. These results encouraged us to synthesize homothymidylate 8-mers with one or two stereodefined PS-linkages (**14a**, **14b**, and **15** in Table 2) based on the synthetic strategy shown in Scheme 1. The *O*⁴-phosphites were removed by adding 0.3 M imidazole to the capping reagents. TBHP was selected as the oxidizing agent on the basis of previous reports in the literature that demonstrated its compatibility with phosphorothioate triesters.^{19,20} DMTr⁺ assays revealed that the average coupling yields were 98%–99%. Reversed-phase HPLC (RP-HPLC) analyses showed that PO/PS-ODNs had been synthesized in a highly stereocontrolled manner without any significant byproducts (Figure 1) and that the targeted products were isolated in diastereopure forms (Figure 2). The diastereopurity of **15** was also confirmed by enzymatic digestion using an experimental process that is described below.

Stereocontrolled Solid-Phase Synthesis of PO/PS-ODNs Using Different Activators in the Phosphoramidite and Oxazaphospholidine Cycles. The previous section described the successful syntheses of *P*-stereodefined PO/PS-ODNs via CMPT-promoted condensation of the phosphoramidite and oxazaphospholidine monomers and cleavage of the

*O*⁴-phosphites with imidazole. However, in the case of ODNs that contained multiple thymines, we had anticipated that the byproducts of *O*⁴-phosphitylation of the thymine bases would not be completely eliminated with imidazole. We thus investigated the synthesis of *P*-stereodefined PO/PS-ODNs with a conventional, highly nucleophilic azole as the activator to prevent *O*⁴-phosphitylation of the phosphoramidite monomers. This method is depicted in Scheme 3, in which two different synthetic cycles employ 5-ethylthio-1*H*-tetrazole (ETT)²¹ and CMPT as activators for the phosphoramidite and oxazaphospholidine monomers, respectively. We had predicted that the *O*⁴-phosphites on the thymine residues would decompose during the condensation step with ETT. The “PO cycle” follows the same steps as the conventional phosphoramidite method: (1) condensation of the phosphoramidites **1a–d** with the 5'-OH of a nucleoside on the solid-support **2** in the presence of ETT to produce phosphite triester intermediates **3**; (2) capping of the unreacted 5'-OH with Pac₂O and *N*-methylimidazole (NMI), followed by oxidation of the phosphite triesters with TBHP to phosphate triesters **4**; and (3) 5'-detritylation by 3% TCA to regenerate 5'-OH. The “PS cycle,” developed for the stereocontrolled synthesis of PS-ODNs,^{12c} consists of the following three steps: (1) condensation of the diastereopure nucleoside 3'-*O*-oxazaphospholidine monomers (Rp)- or (Sp)-**5a–d** with **2** in the presence of CMPT to produce stereospecific phosphite triesters **6**; (2) capping of the unreacted 5'-OH and the secondary amino group of the resultant phosphite intermediates **6** with CF₃COIm and NMI, followed by transformation into the phosphorothioate triester intermediates **7** via sulfurization with 3-phenyl-1,2,4-dithiazoline-5-one (POS);²² and (3) 5'-detritylation. *P*-Stereodefined PO/PS-ODNs are synthesized by switching between these two cycles. The deprotection and release of the resultant oligomers from the solid support are accomplished by treatment with a blend of concentrated aqueous NH₃ and EtOH (5:1, v/v). *P*-Stereodefined PO/PS-ODNs are then obtained from purification by RP-HPLC.

We first synthesized four different types of PO/PS-ODN 8-mers (**16a**, **16b**, **17a**, and **17b**) that possessed either an (Rp)- or an (Sp)-PS-linkage (Table 3, entries 1–4). RP-HPLC analyses showed that all the 8-mers were produced with high coupling efficiency and diastereopurity.¹⁷ PO/PS-ODNs were isolated by RP-HPLC in good yields (29%–62%). We were further motivated to synthesize PO/PS-ODN 12-mers (**18a**, **18b**, **19a**, **19b**, **20a**, and **20b**) with three consecutive (Sp)- or (Rp)-PS-linkages at the internal or terminal regions of the molecule (Table 3, entries 5–10). The RP-HPLC profiles of the crude products (Figure 3) showed that ODNs were efficiently synthesized with a high stereospecificity. The desired 12-mers **18–20** were isolated as major products with good yields (28%–48%) (Figure 4). MALDI-TOF-MS analysis of the

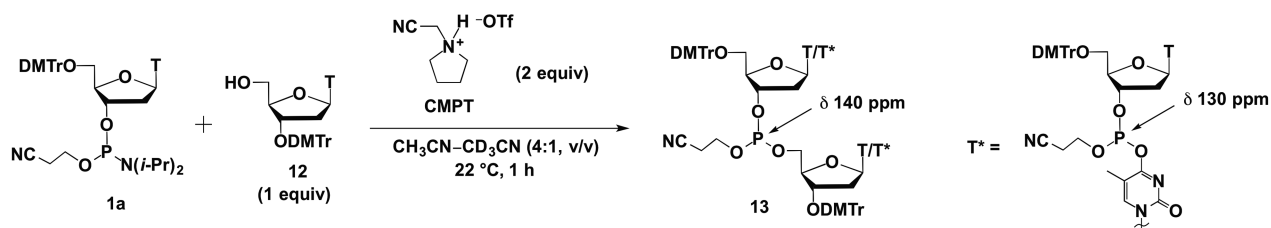
Scheme 2. *O*⁴-Phosphitylation of Thymine in the Presence of CMPT

Table 2. *P*-Stereodefined PO/PS-ODNs 14 and 15, Which Were Synthesized According to Scheme 1

entry	PO/PS-ODN ^a	O.D. ^b	isolated yield (%)	MALDI-TOF-MS	
				calcd.	found
1	(<i>Rp</i>)-d(TTTT _s TTTT) 14a	20	60	2385.4	2386.0
2	(<i>Sp</i>)-d(TTTT _s TTTT) 14b	20	60	2385.4	2386.2
3	all-(<i>Sp</i>)-d(TTTTT _s T _s T) 15	18	54	2401.4	2400.0

^aSubscript "S" = phosphorothioate diester. ^bOverall materials (O.D. = optical density units) measured at 260 nm UV absorption.

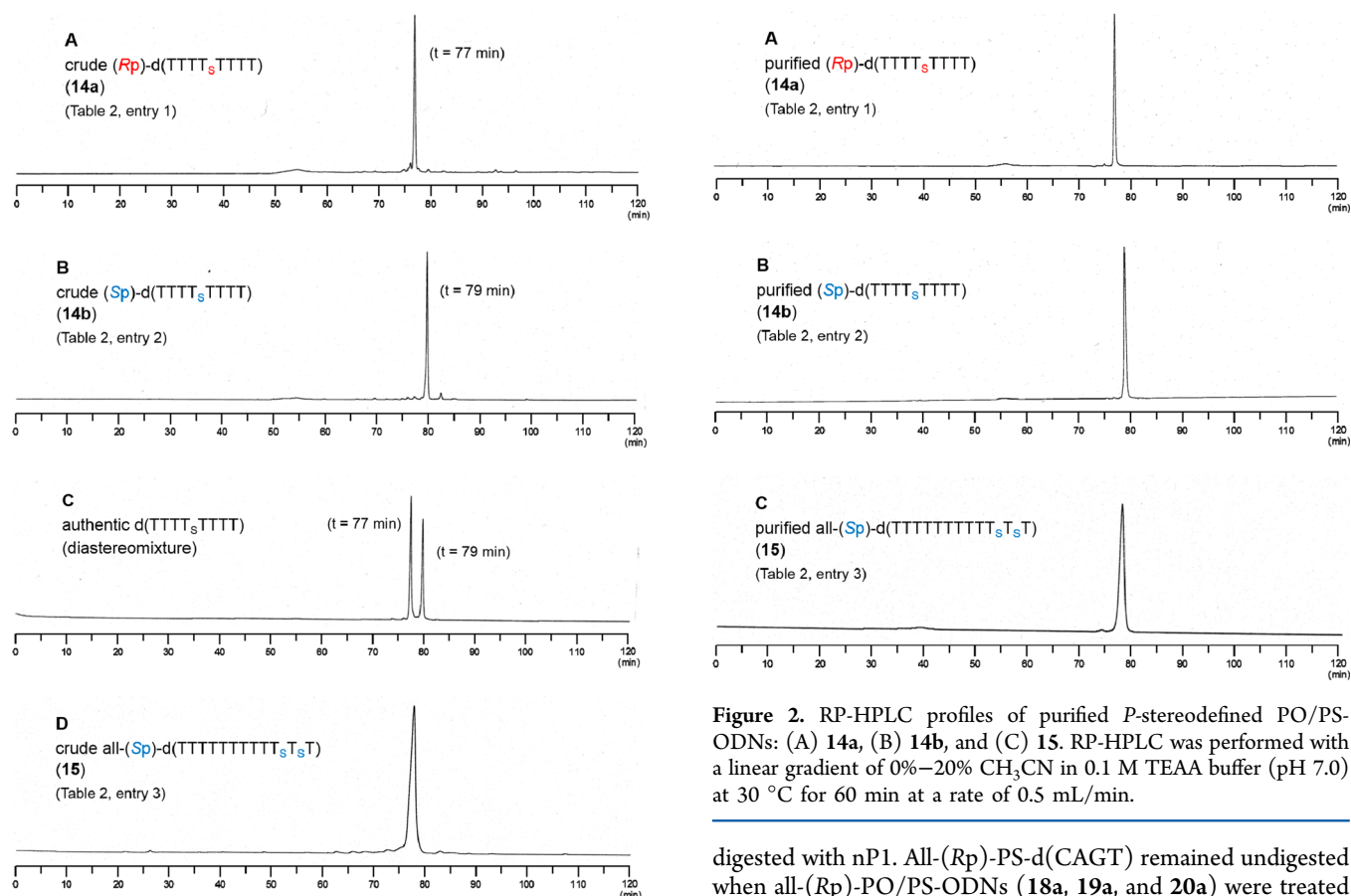


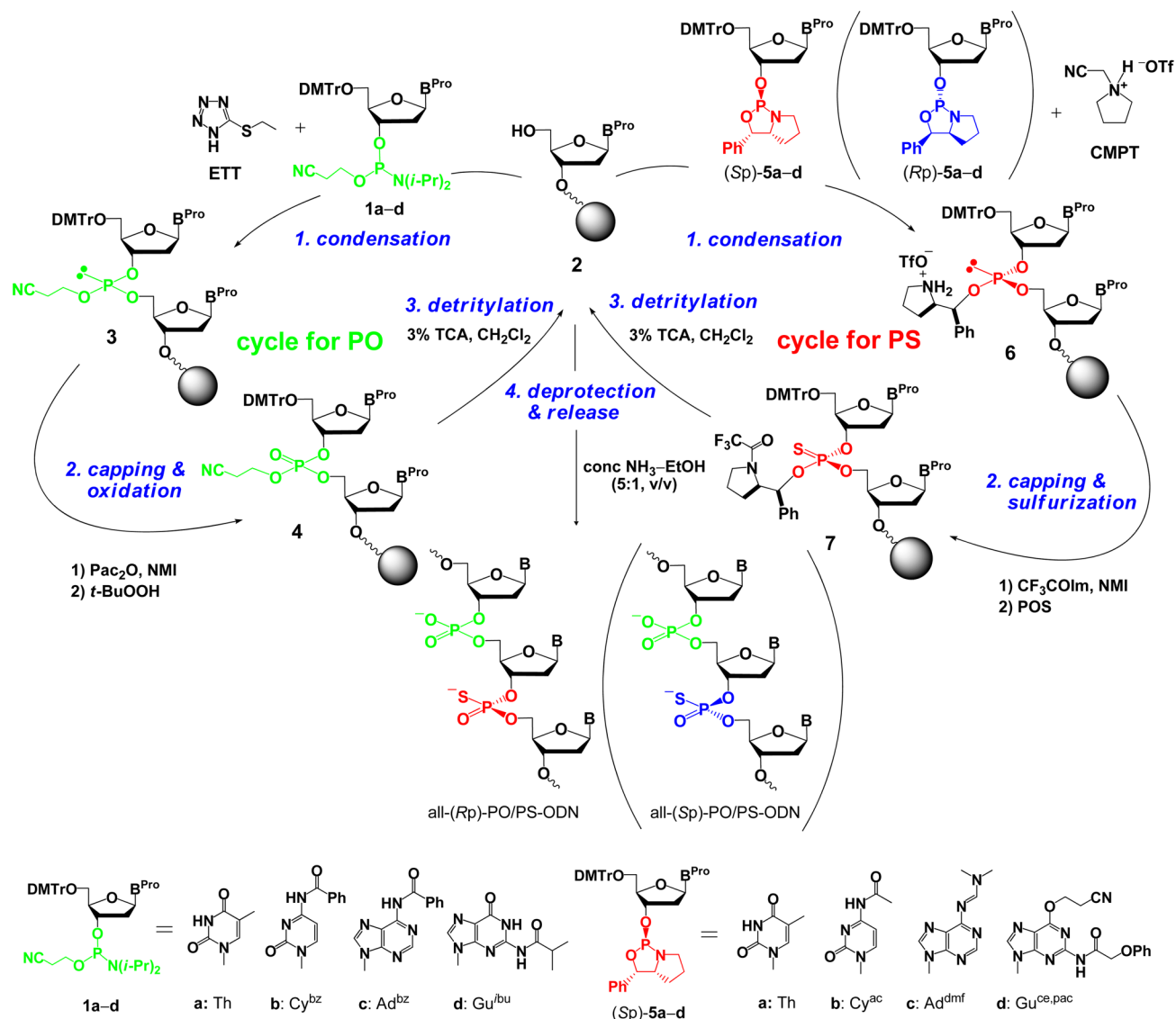
Figure 1. RP-HPLC profiles of crude *P*-stereodefined PO/PS-ODNs: (A) **14a**; (B) **14b**; (C) (*Rp/Sp*)-d(TTTT_sTTTT), the product of a nonstereoselective synthesis (shown as a reference); and (D) **15**. RP-HPLC was performed with a linear gradient of 0%–20% CH₃CN in 0.1 M TEAA buffer (pH 7.0) at 30 °C for 60 min at a rate of 0.5 mL/min.

resultant oligomers showed that none of the PS-linkages were desulfurized during the synthetic process.¹⁷

Enzymatic Digestion of *P*-Stereodefined PO/PS-ODNs. PO/PS-ODNs (**15**, **18a**, **18b**, **19a**, **19b**, **20a**, and **20b**) were digested by nuclease P1²³ (nP1) (*Sp*-specific) and snake venom phosphodiesterase (svPDE)²⁴ (*Rp*-specific) to confirm the stereochemical configurations and diastereopurities of the products. PO/PS-ODNs were analyzed by RP-HPLC after an incubation period of 12 h at 37 °C with nP1 or svPDE (Figures 6 and 7). To reduce any complications within RP-HPLC analyses, alkaline phosphatase was also added to the digestion mixtures to ensure that 5'-phosphorylated PS-d(TTT) or PS-d(CAGT) would not be generated (**19a/20a** + nP1 and **15/19b/20b** + svPDE). Figure 5A and Figure 6D–F show that all-(*Sp*)-PO/PS-ODNs (**15**, **18b**, **19b**, and **20b**) were completely

Figure 2. RP-HPLC profiles of purified *P*-stereodefined PO/PS-ODNs: (A) **14a**, (B) **14b**, and (C) **15**. RP-HPLC was performed with a linear gradient of 0%–20% CH₃CN in 0.1 M TEAA buffer (pH 7.0) at 30 °C for 60 min at a rate of 0.5 mL/min.

digested with nP1. All-(*Rp*)-PS-d(CAGT) remained undigested when all-(*Rp*)-PO/PS-ODNs (**18a**, **19a**, and **20a**) were treated with nP1 (+ alkaline phosphatase) (Figures 6A–C). The ratios of the digestion products obtained from **19a** and **20a** (four kinds of 2'-deoxyribonucleosides and all-(*Rp*)-PS-d(CAGT)) were in agreement with the calculated values (dC:dG:dT:dA:all-(*Rp*)-d(CAGT) = 1.97:2.28:2.00:1.96:1.00 from **19a** (Figure 6B) and 1.95:2.23:2.01:1.88:1.00 from **20a** (Figure 6C), respectively). Conversely, complete digestion was observed when all-(*Rp*)-PO/PS-ODNs (**18a**, **19a**, and **20a**) were treated with svPDE (Figures 7A–C), whereas all-(*Sp*)-PS-d(TTT) and all-(*Sp*)-PS-d(CAGT) remained undigested in the mixtures of all-(*Sp*)-PO/PS-ODNs (**15**, **18b**, **19b**, and **20b**) with svPDE (+ alkaline phosphatase) (Figure 5B and Figure 7D–F). The ratios of hydrolysates obtained from **15**, **19b**, and **20b** were also in agreement with the calculated values (dT:all-(*Sp*)-d(T_sT_sT) = 4.81:1.00 from **15** (Figure 5B), dC:dG:dT:dA:all-(*Sp*)-d(CAGT) = 1.84:2.15:1.94:1.88:1.00 from **19b** (Figure 7B), and 1.67:1.93:1.74:1.67:1.00 from **20b** (Figure 7C), respectively). These experiments verified that the proper stereochemical configurations were obtained for the syntheses of PO/PS-ODNs with oxazaphospholidine monomers **5a–d** since (*Rp*)- and (*Sp*)-PS-linkages were formed from the (*Sp*)- and (*Rp*)-monomers, respectively.^{12c} The diastereopurities of PO/PS-ODNs were also confirmed.

Scheme 3. Synthetic Cycles for *P*-Stereodefined PO/PS-ODNs Using ETT and CMPT as ActivatorsTable 3. *P*-Stereodefined PO/PS-ODN 8–12-mers 16–20 That Were Synthesized According to Scheme 3

entry	PO/PS-ODN ^a	O.D. ^b	isolated yield (%)	MALDI-TOF-MS	
				calcd.	found
1	(<i>Rp</i>)-d(CAGT ₅ CAGT) 16a	27	62	2423.4	2424.2
2	(<i>Sp</i>)-d(CAGT ₅ CAGT) 16b	26	59	2423.4	2425.2
3	(<i>Rp</i>)-d(CG ₅ GCCGCC) 17a	10	29	2385.4	2386.2
4	(<i>Sp</i>)-d(CG ₅ GCCGCC) 17b	11	33	2385.4	2386.1
5	all-(<i>Rp</i>)-d(C ₅ A ₅ G ₅ TCAGTCAGT) 18a	21	31	3690.6	3692.4
6	all-(<i>Sp</i>)-d(C ₅ A ₅ G ₅ TCAGTCAGT) 18b	29	44	3690.6	3692.7
7	all-(<i>Rp</i>)-d(CAGTC ₅ A ₅ G ₅ TCAGT) 19a	19	28	3690.6	3692.4
8	all-(<i>Sp</i>)-d(CAGTC ₅ A ₅ G ₅ TCAGT) 19b	31	47	3690.6	3692.6
9	all-(<i>Rp</i>)-d(CAGTCAGTC ₅ A ₅ G ₅ T) 20a	17	26	3690.6	3692.6
10	all-(<i>Sp</i>)-d(CAGTCAGTC ₅ A ₅ G ₅ T) 20b	32	48	3690.6	3692.6

^aSubscript "S" = phosphorothioate diester. ^bOverall materials (O.D. = optical density units) measured at 260 nm UV absorption.

Hybridization Properties of *P*-Stereodefined PO/PS-ODNs with Complementary ORN. The hybridization properties of the *P*-stereodefined PO/PS-ODN 12-mers (18a, 18b, 19a, 19b, 20a, and 20b) with a complementary ORN were

studied with a UV-melting experiment that used unmodified d(CAGT)₃ 21 as the standard (Figure 8 and Table 4).

The *T*_m values for the PO/PS-ODN duplexes are shown in Table 4. Duplexes with (*Rp*)-PS-linkages (18a, 19a, and 20a)

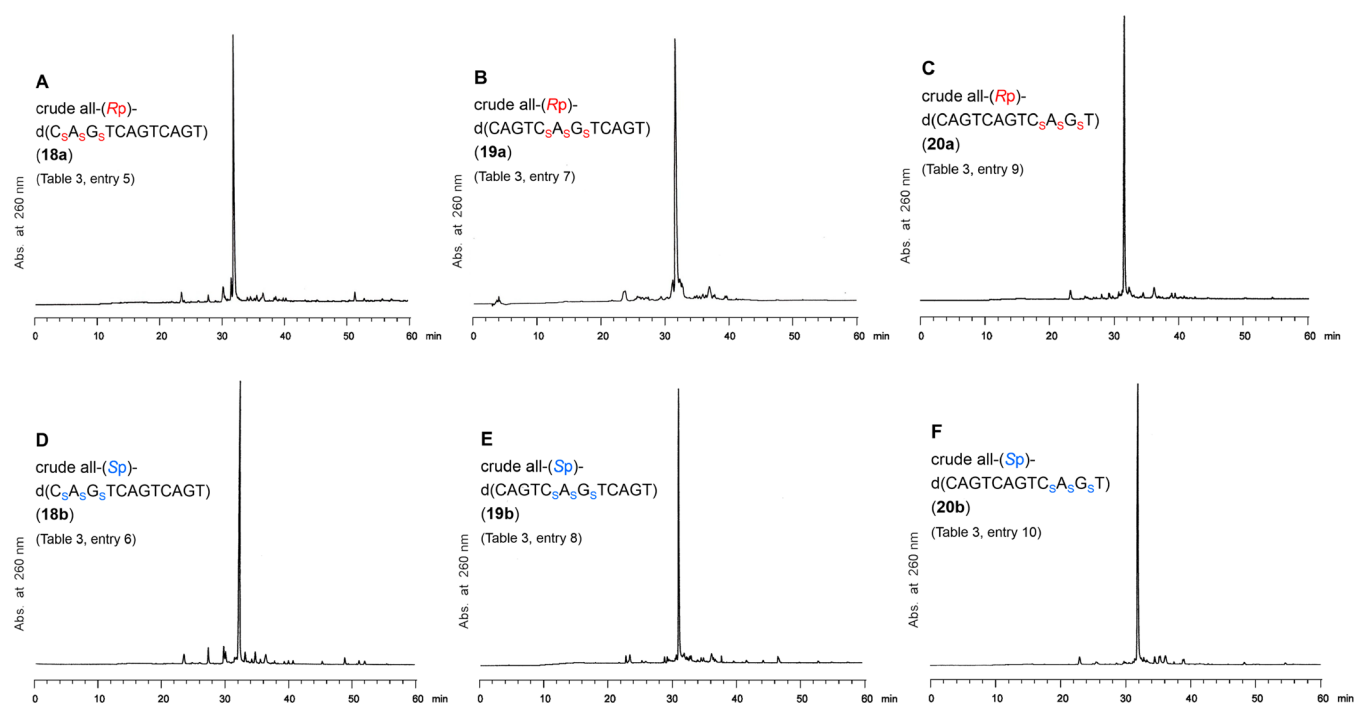


Figure 3. RP-HPLC profiles of crude PO/PS-ODN 12-mers: (A) **18a**, (B) **19a**, (C) **20a**, (D) **18b**, (E) **19b**, and (F) **20b**. RP-HPLC was performed with a linear gradient of 0%–30% CH₃CN in 0.1 M TEAA buffer (pH 7.0) over 60 min at 30 °C at a rate of 0.5 mL/min.

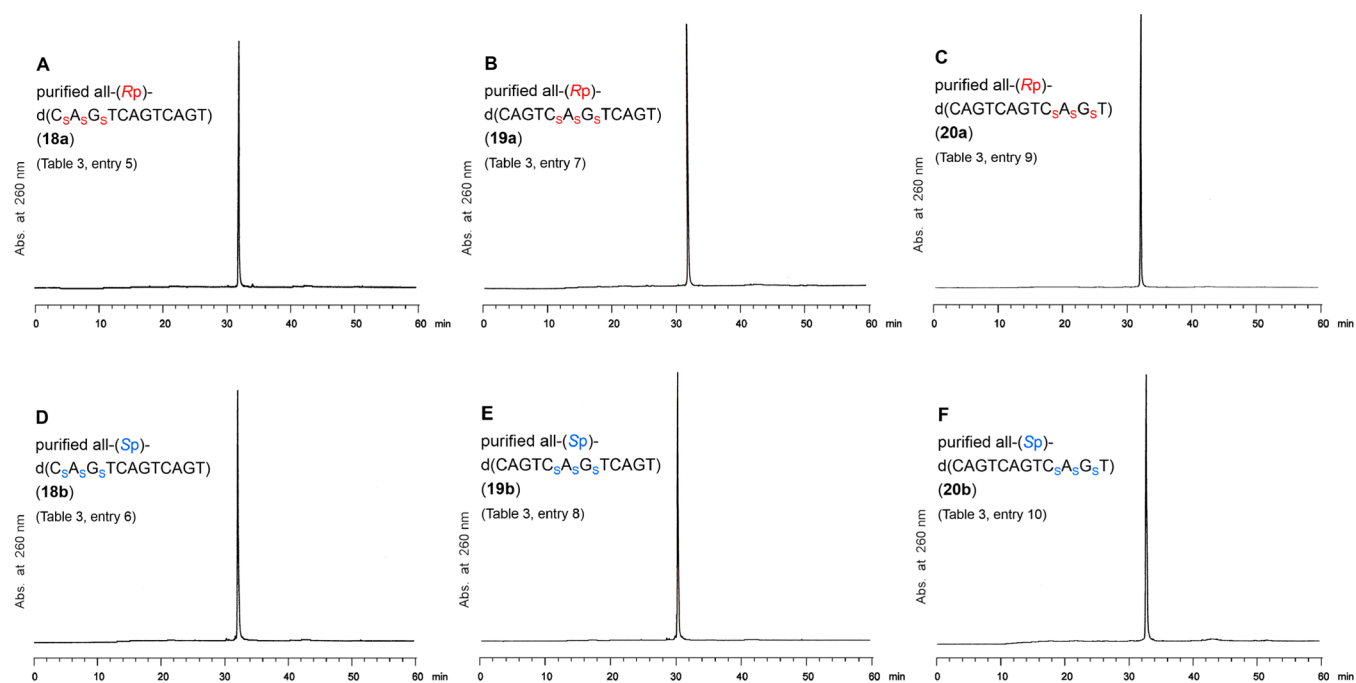


Figure 4. RP-HPLC profiles of purified PO/PS-ODN 12-mers: (A) **18a**, (B) **19a**, (C) **20a**, (D) **18b**, (E) **19b**, and (F) **20b**. RP-HPLC was performed with a linear gradient of 0%–30% CH₃CN in 0.1 M TEAA buffer (pH 7.0) over 60 min at 30 °C at a rate of 0.5 mL/min.

exhibited moderately lower values of T_m than unmodified d(CAGT)₃ **21** ($\Delta T_m = -1.4$ to -1.3 °C or -0.4 °C/PS-linkage); their all-(Sp)-counterparts (**18b**, **19b**, and **20b**) showed even lower values ($\Delta T_m = -3.5$ to -2.4 °C or -1.2 to -0.8 °C/PS-linkage). The decrease in T_m for each modification [(Rp)- or (Sp)-PS-linkage] was very similar to results reported for fully modified PS-ODNs.^{7b} We discovered that the destabilizing effects of (Sp)-PS-linkages were dependent on their location within the molecule. There was a smaller

decrease in T_m when these linkages were incorporated into the terminal regions of the molecule (entries 3 and 7 rather than entry 5 in Table 4). In contrast, the effects of the (Rp)-PS-linkages were not strongly dependent on their location within the molecule (entries 2, 4, and 6).

CONCLUSIONS

We have developed a novel method for the production of *P*-stereodefined PO/PS-ODNs on an automated synthesizer. The

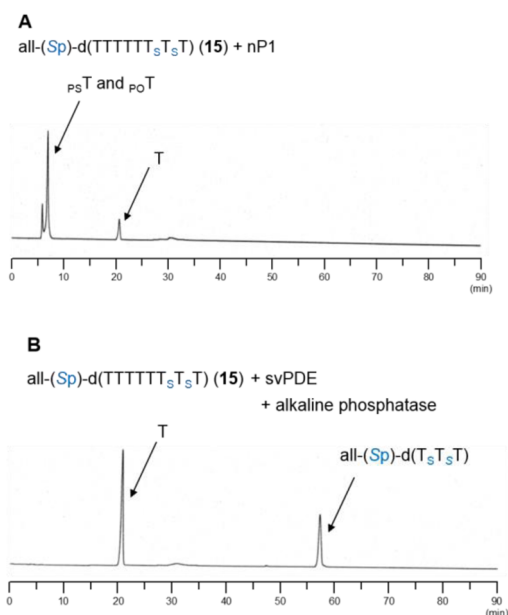


Figure 5. RP-HPLC profiles of reaction mixtures obtained through the digestion of purified **15** with (A) nP1 and (B) svPDE and alkaline phosphatase. RP-HPLC was performed with a linear gradient of 0%–20% CH₃CN in 0.1 M TEAA buffer (pH 7.0) over 90 min at 50 °C at a rate of 0.5 mL/min.

conventional phosphoramidite method was integrated into the oxazaphospholidine method that we had previously developed for the stereocontrolled synthesis of *P*-chiral oligonucleotides. *P*-Stereodefined PO/PS-ODNs that possess multiple PS-linkages at targeted positions were efficiently synthesized with a high degree of stereoselectivity. A thermal denaturation study compared the T_m values for an unmodified ODN–ORN duplex

with those for duplexes formed from all-(*Rp*)-PO/PS-ODNs and the complementary ORN; the T_m decreased by 0.4 °C for every modification. Conversely, the T_m values of their all-(*Sp*)-counterparts were lower than the unmodified standard by 0.8 to 1.2 °C for every modification. The destabilizing effect of the (*Sp*)-PS-linkages was smaller when they were located in the terminal regions of the molecule. The effects of the (*Rp*)-PS-linkages were largely independent of their locations within the molecule.

EXPERIMENTAL SECTION

A General Procedure for the Stereocontrolled Solid-Phase Synthesis of PO/PS-ODNs that Uses CMPT as an Activator for Both Phosphoramidite and Oxazaphospholidine Monomers (14a, 14b, and 15). The automated solid-phase synthesis of *P*-stereodefined PO/PS-ODNs (**14a**, **14b**, and **15**) with 5'-*O*-DMTr-thymidine-loaded HCP (0.5 μmol) was performed according to the procedure given in Table 5. The chain was elongated by repeating steps 1–8 in Table 5, and the 5'-*O*-DMTr group was subsequently removed with 3% TCA in CH₂Cl₂. The deprotection of both the nucleobases and the PO/PS-linkages, along with the cleavage of the linker, was accomplished with a 1 mL blend of 25% NH₃ aqueous solution and EtOH (5:1, v/v) for 12–48 h at 55 °C. The resultant crude products were analyzed or purified by RP-HPLC. The fractions that contained the targeted PO/PS-ODN were collected and lyophilized. Overall materials (O.D. = optical density units, weight (triethylammonium salt)) and isolated yields were determined by UV quantitation at 260 nm. (*Rp*)-d(TTTT₅TTTT) **14a**, 20 O.D., 0.93 mg, 60% yield, MALDI-TOF-MS: m/z calcd for C₈₀H₁₀₄N₁₆O₅₃P₇S⁻ [(M - H)⁻] 2385.4, found 2386.0. (*Sp*)-d(TTTT₅TTTT) **14b**, 20 O.D., 0.93 mg, 60% yield, MALDI-TOF-MS: m/z calcd for C₈₀H₁₀₄N₁₆O₅₃P₇S⁻ [(M - H)⁻] 2385.4, found 2386.2. All-(*Sp*)-d(TTTTTT₅T₅T) **15**, 18 O.D., 0.84 mg, 54% yield, MALDI-TOF-MS: m/z calcd for C₈₀H₁₀₄N₁₆O₅₃P₇S⁻ [(M - H)⁻] 2401.4, found 2400.0.

A General Procedure for the Stereocontrolled Solid-Phase Synthesis of PO/PS-ODNs that Uses ETT and CMPT as Activators (16–20a,b). The automated solid-phase synthesis of *P*-

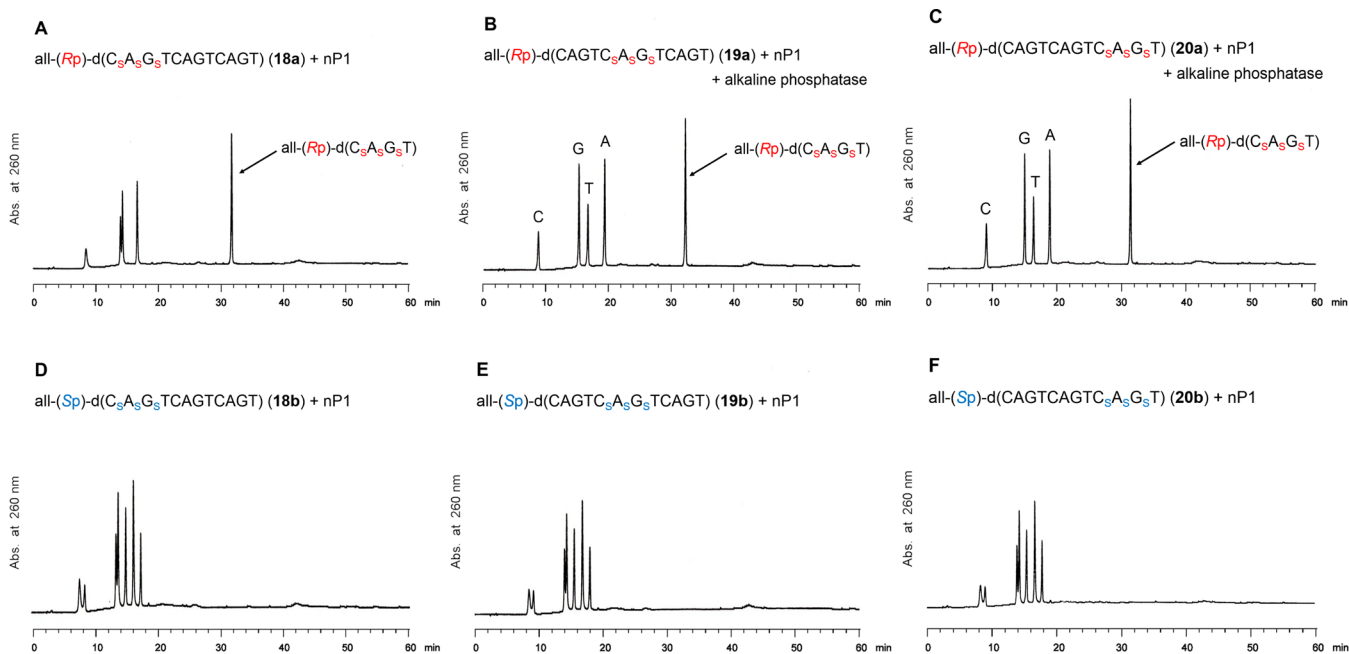


Figure 6. RP-HPLC profiles of reaction mixtures obtained through the digestion of purified all-(*Rp*)- and all-(*Sp*)-PO/PS-ODN 12-mers with nP1: (A) **18a** with nP1, (B) **19a** with nP1 and alkaline phosphatase, (C) **20a** with nP1 and alkaline phosphatase, (D) **18b** with nP1, (E) **19b** with nP1, and (F) **20b** with nP1; RP-HPLC was performed with a linear gradient of 0%–30% CH₃CN in 0.1 M TEAA buffer (pH 7.0) over 60 min at 30 °C at a rate of 0.5 mL/min.

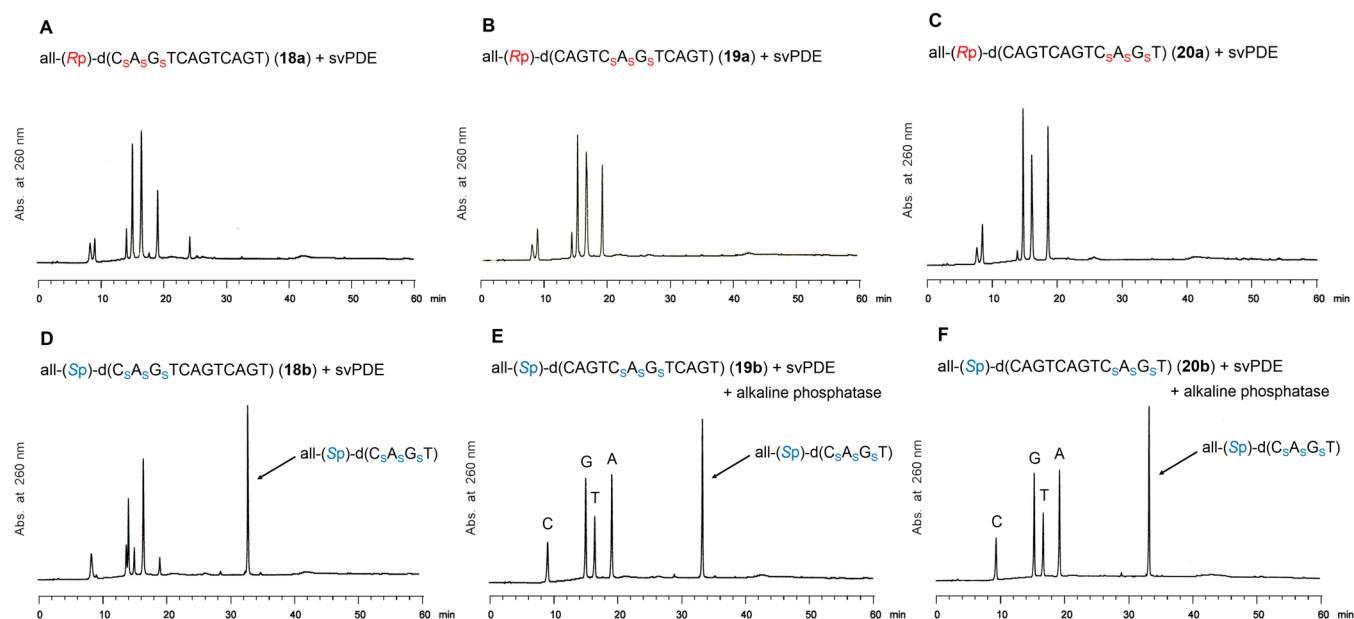


Figure 7. RP-HPLC profiles of reaction mixtures obtained through the digestion of purified all-(Rp)- and all-(Sp)-PO/PS-ODN 12-mers with svPDE: (A) **18a** with svPDE, (B) **19a** with svPDE, (C) **20a** with svPDE, (D) **18b** with svPDE, (E) **19b** with svPDE and alkaline phosphatase, and (F) **20b** with svPDE and alkaline phosphatase. RP-HPLC was performed with a linear gradient of 0%–30% CH₃CN in 0.1 M TEAA buffer (pH 7.0) over 60 min at 30 °C at a rate of 0.5 mL/min.

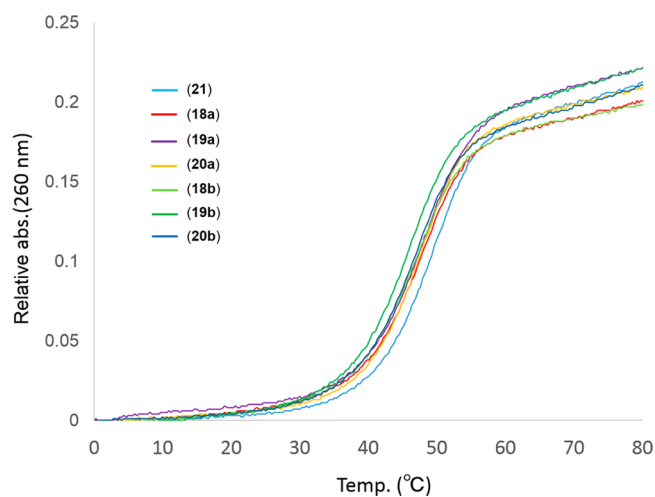


Figure 8. UV-melting curves for the duplexes of *P*-stereodefined PO/PS-ODN 12-mers with r(ACUG)₃. The buffer conditions were 10 mM sodium phosphate (pH 7.0) and 100 mM NaCl.

stereodefined PO/PS-ODNs with 5'-O-DMTr-thymidine-loaded HCP (0.5 μmol) was performed according to the procedure given in Table 6. The chain was elongated by repeating steps 1–8 in Table 6, and the 5'-O-DMTr group was subsequently removed with 3% TCA in CH₂Cl₂. The deprotection of both the nucleobases and the PO/PS-linkages, along with the cleavage of the linker, was accomplished with a 6 mL blend of 25% NH₃ aqueous solution and EtOH (5:1, v/v) for 12 h at 30 °C. The resultant crude products were purified by RP-HPLC. Fractions that contained the targeted PO/PS-ODN were collected and lyophilized. Overall materials (O.D. = optical density units) and isolated yields were determined by UV quantitation at 260 nm.²⁵ (Rp)-d(CAGT₅CAGT) **16a**, 27 O.D., 0.97 mg, 62% yield, MALDI-TOF-MS: *m/z* calcd for C₇₈H₉₈N₃₀O₄₅P₇S⁻ [(M - H)⁻] 2423.4, found 2424.2. (Sp)-d(CAGT₅CAGT) **16b**, 26 O.D., 0.92 mg, 59% yield, MALDI-TOF-MS: *m/z* calcd for C₇₈H₉₈N₃₀O₄₅P₇S⁻ [(M - H)⁻] 2423.4, found 2425.2. (Rp)-d(CG₅GCCGCC) **17a**, 10 O.D., 0.49 mg, 29% yield, MALDI-TOF-MS: *m/z* calcd for C₇₅H₉₆N₃₀O₄₅P₇S⁻ [(M - H)⁻] 2385.4, found 2386.2. (Sp)-d(CG₅GCCGCC) **17b**, 11 O.D., 0.51 mg, 33% yield, MALDI-TOF-MS: *m/z* calcd for C₇₅H₉₆N₃₀O₄₅P₇S⁻ [(M - H)⁻] 2385.4, found 2386.1. All-(Rp)-d(C₅A₅G₅TCAGTCAGT) **18a**, 21 O.D., 0.75 mg, 31% yield, MALDI-TOF-MS: *m/z* calcd for C₁₁₇H₁₄₇N₄₅O₆₇P₁₁S₃⁻ [(M - H)⁻] 3690.6, found 3692.4. All-(Sp)-d(C₅A₅G₅TCAGTCAGT) **18b**, 29 O.D., 1.06

Table 4. *T_m*-Values for the Duplexes of *P*-Stereodefined PO/PS-ODN 12-mers with r(ACUG)₃

entry	ODN	PO/PS-ODN/r(ACUG) ₃	
		<i>T_m</i> (°C) ^a	Δ <i>T_m</i> (°C) ^b
1	unmodified d(CAGT) ₃ 21	45.3 ± 0.3	–
2	all-(Rp)-d(C ₅ A ₅ G ₅ TCAGTCAGT) 18a	44.0 ± 0.3	–1.3
3	all-(Sp)-d(C ₅ A ₅ G ₅ TCAGTCAGT) 18b	42.9 ± 0.3	–2.4
4	all-(Rp)-d(CAGTC ₅ A ₅ G ₅ TCAGT) 19a	44.0 ± 0.1	–1.3
5	all-(Sp)-d(CAGTC ₅ A ₅ G ₅ TCAGT) 19b	41.8 ± 0.1	–3.5
6	all-(Rp)-d(CAGTCAGTC ₅ A ₅ G ₅ T) 20a	43.9 ± 0.1	–1.4
7	all-(Sp)-d(CAGTCAGTC ₅ A ₅ G ₅ T) 20b	42.8 ± 0.1	–2.5

^aAverage values of the experiment in triplicate. ^bThe difference in *T_m* relative to unmodified d(CAGT)₃ **21**.

Table 5. Procedure for the Automated Solid-Phase Synthesis of PO/PS-ODNs with CMPT as an Activator

step	operation	cycle for PO		cycle for PS	
		reagents	time	reagents	time
1	detritylation	3% (w/v) TCA in CH ₂ Cl ₂	49 s	3% (w/v) TCA in CH ₂ Cl ₂	49 s
2	washing	dry CH ₃ CN	–	dry CH ₃ CN	–
3	condensation	0.1 M monomer 1a and 0.5 M CMPT in dry CH ₃ CN	5 min	0.1 M monomer 5a and 0.5 M CMPT in dry CH ₃ CN	5 min
4	washing	dry CH ₃ CN	–	dry CH ₃ CN	–
5	capping	0.5 M CF ₃ COIm, 1.0 M DMAN, and 0.3 M Im in dry THF	15 s	0.5 M CF ₃ COIm, 1.0 M DMAN, and 0.3 M Im in dry THF	15 s
6	washing	dry CH ₃ CN	–	dry CH ₃ CN	–
7	oxidation/sulfurization	1 M <i>t</i> -BuOOH in dry toluene	2 min	0.3 M DTD in dry CH ₃ CN	6 min
8	washing	dry CH ₃ CN	–	dry CH ₃ CN	–

Table 6. Procedure for the Automated Solid-Phase Synthesis of PO/PS-ODNs with ETT and CMPT as Activators

step	operation	cycle for PO		cycle for PS	
		reagents	time	reagents	time
1	detritylation	3% (w/v) TCA in CH ₂ Cl ₂	12 s	3% (w/v) TCA in CH ₂ Cl ₂	12 s
2	washing	dry CH ₃ CN	–	dry CH ₃ CN	–
3	condensation	0.1 M monomer 1a–d and 0.25 M ETT in dry CH ₃ CN	30 s	0.1 M monomer 5a–d and 0.5 M CMPT in dry CH ₃ CN	5 min
4	washing	dry CH ₃ CN	–	dry CH ₃ CN	–
5	capping	Pac ₂ O and 16% (v/v) NMI in dry THF	40 s	0.5 M CF ₃ COIm and 16% (v/v) NMI in dry THF	40 s
6	washing	dry CH ₃ CN	–	dry CH ₃ CN	–
7	oxidation/sulfurization	1 M <i>t</i> -BuOOH in dry toluene	30 s	0.3 M POS in dry CH ₃ CN	8 min
8	washing	dry CH ₃ CN	–	dry CH ₃ CN	–

mg, 44% yield, MALDI-TOF-MS: m/z calcd for C₁₁₇H₁₄₇N₄₅O₆₇P₁₁S₃[–] [(M – H)[–]] 3690.6, found 3692.7. All-(Rp)-d(CAGTC₅A₅G₅TCAGT) **19a**, 19 O.D., 0.67 mg, 28% yield, MALDI-TOF-MS: m/z calcd for C₁₁₇H₁₄₇N₄₅O₆₇P₁₁S₃[–] [(M – H)[–]] 3690.6, found 3692.4. All-(Sp)-d(CAGTC₅A₅G₅TCAGT) **19b**, 31 O.D., 1.13 mg, 47% yield, MALDI-TOF-MS: m/z calcd for C₁₁₇H₁₄₇N₄₅O₆₇P₁₁S₃[–] [(M – H)[–]] 3690.6, found 3692.6. All-(Rp)-d(CAGTCAGTC₅A₅G₅T) **20a**, 17 O.D., 0.62 mg, 26% yield, MALDI-TOF MS: m/z calcd for C₁₁₇H₁₄₇N₄₅O₆₇P₁₁S₃[–] [(M – H)[–]] 3690.6, found 3692.6. All-(Sp)-d(CAGTCAGTC₅A₅G₅T) **20b**, 32 O.D., 1.15 mg, 48% yield, MALDI-TOF-MS: m/z calcd for C₁₁₇H₁₄₇N₄₅O₆₇P₁₁S₃[–] [(M – H)[–]] 3690.6, found 3692.6.

Enzymatic Digestion of P-Stereodefined PO/PS-ODNs. *Digestion of PO/PS-ODN (15) with nP1.* An aqueous solution (200 μL, pH 7.2) comprising purified **15** (2.0 nmol), nuclease P1 from *Penicillium citrinum* (4 units), 100 mM Tris–HCl, and 1 mM ZnCl₂ was incubated for 12 h at 37 °C. The mixture was heated at 100 °C for 1 min to inactivate the enzyme. The solution was then filtered and analyzed by RP-HPLC.

Digestion of PO/PS-ODNs (18a, 18b, 19b, and 20b) with nP1. An aqueous solution (100 μL, pH 7.2) comprising a purified PO/PS-ODN (1.0 nmol), nuclease P1 from *Penicillium citrinum* (2 units), 100 mM Tris–HCl, and 1 mM ZnCl₂ was incubated for 12 h at 37 °C. The mixture was diluted with 0.1 M TEAA buffer (100 μL, pH 7.0) and heated at 100 °C for 1 min to inactivate the enzyme. The solution was then filtered and analyzed by RP-HPLC.

Digestion of PO/PS-ODNs (19a and 20a) with nP1. An aqueous solution (100 μL, pH 7.2) comprising purified PO/PS-ODN (1.0 nmol), nuclease P1 from *Penicillium citrinum* (2 units), 100 mM Tris–HCl, alkaline phosphatase from calf intestine (0.4 units), and 1 mM ZnCl₂ was incubated for 12 h at 37 °C. The mixture was diluted with 0.1 M TEAA buffer (100 μL, pH 7.0) and heated at 100 °C for 1 min to inactivate the enzymes. The solution was then filtered and analyzed by RP-HPLC.

Digestion of PO/PS-ODN (15) with svPDE. An aqueous solution (200 μL, pH 8.6) comprising a purified PO/PS-ODN (2.0 nmol), svPDE from *Crotalus adamanteus* (8.0 × 10^{–3} units), alkaline phosphatase from calf intestine (0.8 units), 100 mM Tris–HCl, and 15 mM MgCl₂ was incubated for 12 h at 37 °C. The mixture was then

heated for 1 min at 100 °C to inactivate the enzymes. The solution was then filtered and analyzed by RP-HPLC.

Digestion of PO/PS-ODNs (18a, 18b, 19a, and 20a) with svPDE. An aqueous solution (100 μL, pH 8.6) comprising purified PO/PS-ODN (1.0 nmol), svPDE from *Crotalus adamanteus* (4.0 × 10^{–3} units), 100 mM Tris–HCl, and 15 mM MgCl₂ was incubated for 12 h at 37 °C. The mixture was diluted with 0.1 M TEAA buffer (100 μL, pH 7.0) and heated for 1 min at 100 °C to inactivate the enzyme. The solution was then filtered and analyzed by RP-HPLC.

Digestion of PO/PS-ODNs (19b and 20b) with svPDE. An aqueous solution (100 μL, pH 8.6) comprising purified PO/PS-ODN (1.0 nmol), svPDE from *Crotalus adamanteus* (4.0 × 10^{–3} units), alkaline phosphatase from calf intestine (0.4 units), 100 mM Tris–HCl, and 15 mM MgCl₂ was incubated for 12 h at 37 °C. The mixture was diluted with 0.1 M TEAA buffer (100 μL, pH 7.0) and heated for 1 min at 100 °C to inactivate the enzymes. The solution was then filtered and analyzed by RP-HPLC.

Thermal Denaturation Study. An aqueous solution (150 μL, pH 7.0) comprising a 1:1 ratio of ODN (**18–21**) and r(ACUG)₃ (0.30 nmol each), 10 mM phosphate, and 100 mM NaCl was heated from rt to 90 °C. The solution was maintained at 90 °C for 10 min and then cooled at a rate of –1 °C/min from 90 to 10 °C to hybridize the oligomers. The solution was kept at 0 °C for 30 min and then gradually heated for denaturation experiments. The UV absorbance values (at 260 nm) were recorded at 0.5 °C intervals, while the temperature was ramped at a rate of 0.5 °C/min from 0 to 80 °C under Ar.

■ ASSOCIATED CONTENT

📄 Supporting Information

The Supporting Information is available free of charge on the ACS Publications website at DOI: 10.1021/acs.joc.5b02793.

³¹P NMR analyses of O⁴-phosphitylation and desulfurization, HPLC profiles, and MALDI-TOF-MS spectra (PDF)

■ AUTHOR INFORMATION

Corresponding Author

*E-mail: twada@rs.tus.ac.jp.

Notes

The authors declare no competing financial interest.

■ ACKNOWLEDGMENTS

This research was supported by grants from the Core Research for Evolutional Science and Technology (CREST) and the Japan Science and Technology Agency (JST).

■ REFERENCES

- (1) (a) Levin, A. A. *Biochim. Biophys. Acta, Gene Struct. Expression* **1999**, *1489*, 69–84. (b) Eckstein, F. *Antisense Nucleic Acid Drug Dev.* **2000**, *10*, 117–121. (c) Zon, G. *New J. Chem.* **2010**, *34*, 795–804. (d) Guga, P.; Koziolkiewicz, M. *Chem. Biodiversity* **2011**, *8*, 1642–1681.
- (2) (a) Dirin, M.; Winkler, J. *Expert Opin. Biol. Ther.* **2013**, *13*, 875–888. (b) Sharma, V. K.; Sharma, R. K.; Singh, S. K. *MedChemComm* **2014**, *5*, 1454–1471.
- (3) (a) Stein, C. A.; Subasinghe, C.; Shinozuka, K.; Cohen, J. S. *Nucleic Acids Res.* **1988**, *16*, 3209–3221. (b) Soreq, H.; Patinkin, D.; Lev-Lehman, E.; Grifman, M.; Ginzberg, D.; Eckstein, F.; Zakut, H. *Proc. Natl. Acad. Sci. U. S. A.* **1994**, *91*, 7907–7911. (c) Zhang, R.; Iyer, R. P.; Yu, D.; Tan, W.; Zhang, X.; Lu, Z.; Zhao, H.; Agrawal, S. J. *Pharmacol. Exp. Ther.* **1996**, *278*, 971–979. (d) Agrawal, S.; Jiang, Z.; Zhao, Q.; Shaw, D.; Cai, Q.; Roskey, A.; Channavajjala, L.; Saxinger, C.; Zhang, R. *Proc. Natl. Acad. Sci. U. S. A.* **1997**, *94*, 2620–2625. (e) Galderisi, U.; Di Bernardo, G.; Melone, M. A. B.; Galano, G.; Cascino, A.; Giordano, A.; Cipollaro, M. *J. Cell. Biochem.* **1999**, *74*, 31–37.
- (4) Guga, P. *Curr. Top. Med. Chem.* **2007**, *7*, 695–713.
- (5) (a) Stec, W. J.; Zon, G. *Tetrahedron Lett.* **1984**, *25*, 5275–5278. (b) Stec, W. J.; Zon, G.; Egan, W. *J. Am. Chem. Soc.* **1984**, *106*, 6077–6079. (c) Stec, W. J.; Zon, G.; Uznanski, B. *J. Chromatogr.* **1985**, *326*, 263–280. (d) LaPlanche, L. A.; James, T. L.; Powell, C.; Wilson, W. D.; Uznanski, B.; Stec, W. J.; Summers, M. F.; Zon, G. *Nucleic Acids Res.* **1986**, *14*, 9081–9083. (e) Murakami, A.; Tamura, Y.; Wada, H.; Makino, K. *Anal. Biochem.* **1994**, *223*, 285–290. (f) Kanaori, K.; Tamura, Y.; Wada, T.; Nishi, M.; Kanehara, H.; Morii, T.; Tajima, K.; Makino, K. *Biochemistry* **1999**, *38*, 16058–16066.
- (6) (a) Cosstick, R.; Eckstein, F. *Biochemistry* **1985**, *24*, 3630–3638. (b) Wozniak, L. A.; Góra, M.; Bukowiecka-Matusiak, M.; Mourgues, S.; Pratiel, G.; Meunier, B.; Stec, W. J. *Eur. J. Org. Chem.* **2005**, *2005*, 2924–2930. (c) Nawrot, B.; Rebowska, B.; Cieślińska, K.; Stec, W. J. *Tetrahedron Lett.* **2005**, *46*, 6641–6644. (d) Hayakawa, Y.; Hirabayashi, Y.; Hyodo, M.; Yamashita, S.; Matsunami, T.; Cui, D.-M.; Kawai, R.; Kodama, H. *Eur. J. Org. Chem.* **2006**, *2006*, 3834–3844. (e) Nawrot, B.; Widera, K.; Wojcik, M.; Rebowska, B.; Nowak, G.; Stec, W. J. *FEBS J.* **2007**, *274*, 1062–1072.
- (7) (a) Benimetskaya, L.; Tonkinson, J. L.; Koziolkiewicz, M.; Karwowski, B.; Guga, P.; Zeltser, R.; Stec, W.; Stein, C. A. *Nucleic Acids Res.* **1995**, *23*, 4239–4245. (b) Boczkowska, M.; Guga, P.; Stec, W. J. *Biochemistry* **2002**, *41*, 12483–12487. (c) Krieg, A. M.; Guga, P.; Stec, W. J. *Oligonucleotides* **2003**, *13*, 491–499. (d) Wójcik, M.; Cieślak, M.; Stec, W. J.; Goding, J. W.; Koziolkiewicz, M. *Oligonucleotides* **2007**, *17*, 134–145. (e) Pruzan, R.; Zielinska, D.; Rebowska-Koccon, B.; Nawrot, B.; Gryaznov, S. M. *New J. Chem.* **2010**, *34*, 870–874.
- (8) Yu, D.; Kandimalla, E. R.; Roskey, A.; Zhao, Q.; Chen, L.; Chen, J.; Agrawal, S. *Bioorg. Med. Chem.* **2000**, *8*, 275–284.
- (9) Wilk, A.; Grajkowski, A.; Phillips, L. R.; Beaucage, S. L. *J. Am. Chem. Soc.* **2000**, *122*, 2149–2156.
- (10) (a) Stec, W. J.; Grajkowski, A.; Koziolkiewicz, M.; Uznanski, B. *Nucleic Acids Res.* **1991**, *19*, 5883–5888. (b) Stec, W. J.; Grajkowski, A.; Kobylńska, A.; Karwowski, B.; Koziolkiewicz, M.; Misiura, K.; Okruszek, A.; Wilk, A.; Guga, P.; Boczkowska, M. *J. Am. Chem. Soc.* **1995**, *117*, 12019–12029. (c) Stec, W. J.; Karwowski, B.; Boczkowska, M.; Guga, P.; Koziolkiewicz, M.; Sochacki, M.; Wieczorek, M. W.; Blaszczyk, J. *J. Am. Chem. Soc.* **1998**, *120*, 7156–7167. (d) Guga, P.; Okruszek, A.; Stec, W. J. *Top. Curr. Chem.* **2002**, *220*, 169–200. (e) Radzikowska, E.; Baraniak, J. *Org. Biomol. Chem.* **2015**, *13*, 269–276.
- (11) (a) Beaucage, S. L.; Caruthers, M. H. *Tetrahedron Lett.* **1981**, *22*, 1859–1862. (b) McBride, L. J.; Caruthers, M. H. *Tetrahedron Lett.* **1983**, *24*, 245–248. (c) Sinha, N. D.; Biernat, J.; Köster, H. *Tetrahedron Lett.* **1983**, *24*, 5843–5846. (d) Beaucage, S. L.; Iyer, R. P. *Tetrahedron* **1992**, *48*, 2223–2311.
- (12) (a) Oka, N.; Wada, T.; Saigo, K. *J. Am. Chem. Soc.* **2002**, *124*, 4962–4963. (b) Oka, N.; Wada, T.; Saigo, K. *J. Am. Chem. Soc.* **2003**, *125*, 8307–8317. (c) Oka, N.; Yamamoto, M.; Sato, T.; Wada, T. *J. Am. Chem. Soc.* **2008**, *130*, 16031–16037. (d) Iwamoto, N.; Oka, N.; Sato, T.; Wada, T. *Angew. Chem., Int. Ed.* **2009**, *48*, 496–499. (e) Oka, N.; Kondo, T.; Fujiwara, S.; Maizuru, Y.; Wada, T. *Org. Lett.* **2009**, *11*, 967–970. (f) Oka, N.; Wada, T. *Chem. Soc. Rev.* **2011**, *40*, 5829–5843. (g) Nukaga, Y.; Yamada, K.; Ogata, T.; Oka, N.; Wada, T. *J. Org. Chem.* **2012**, *77*, 7913–7922. (h) Nukaga, Y.; Takemura, T.; Iwamoto, N.; Oka, N.; Wada, T. *RSC Adv.* **2015**, *5*, 2392–2395.
- (13) Wan, W. B.; Migawa, M. T.; Vasquez, G.; Murray, H. M.; Nichols, J. G.; Gaus, H.; Berdeja, A.; Lee, S.; Hart, C. E.; Lima, W. F.; Swayze, E. E.; Seth, P. P. *Nucleic Acids Res.* **2014**, *42*, 13456–13468.
- (14) (a) Engels, J.; Jäger, A. *Angew. Chem., Int. Ed. Engl.* **1982**, *21*, 912–913. (b) Hayakawa, Y.; Uchiyama, M.; Noyori, R. *Tetrahedron Lett.* **1986**, *27*, 4191–4194. (c) .
- (15) Song, Q.; Wang, Z.; Sanghvi, Y. S. *Nucleosides, Nucleotides Nucleic Acids* **2003**, *22*, 629–633.
- (16) (a) Barone, A. D.; Tang, J.-Y.; Caruthers, M. H. *Nucleic Acids Res.* **1984**, *12*, 4051–4061. (b) Pon, R. T.; Damha, M. J.; Ogilvie, K. K. *Nucleic Acids Res.* **1985**, *13*, 6447–6465. (c) Oka, N.; Morita, Y.; Itakura, Y.; Ando, K. *Chem. Commun.* **2013**, *49*, 11503–11505.
- (17) See the [Supporting Information](#).
- (18) Addition of nucleophiles (e.g., pyridine hydrochloride and aniline, 1H-tetrazole, benzimidazole triflate in MeOH, and 1-hydroxy-6-nitrobenzotriazole) has been used to remove N-phosphitylation products from nucleobase amino groups in the synthesis of oligonucleotides without base protection (a) Gryaznov, S. M.; Letsinger, R. L. *J. Am. Chem. Soc.* **1991**, *113*, 5876–5877. (b) Gryaznov, S. M.; Letsinger, R. L. *Nucleic Acids Res.* **1992**, *20*, 1879–1882. (c) Hayakawa, Y.; Kataoka, M. *J. Am. Chem. Soc.* **1998**, *120*, 12395–12401. (d) Ohkubo, A.; Kuwayama, Y.; Kudo, T.; Tsunoda, H.; Seio, K.; Sekine, M. *Org. Lett.* **2008**, *10*, 2793–2796.
- (19) Tosquellas, G.; Bologna, J. C.; Morvan, F.; Rayner, B.; Imbach, J.-L. *Bioorg. Med. Chem. Lett.* **1998**, *8*, 2913–2918.
- (20) We also confirmed that the phosphorothioate triester linkages bearing the chiral auxiliary (Scheme 1, 7) was not affected by prolonged treatment with TBHP. See the [Supporting Information](#).
- (21) Wincott, F.; DiRenzo, A.; Shaffer, C.; Grimm, S.; Tracz, D.; Workman, C.; Sweedler, D.; Gonzalez, C.; Scaringe, S.; Usman, N. *Nucleic Acids Res.* **1995**, *23*, 2677–2684.
- (22) Ponomarov, O.; Laws, A. P.; Hanusek, J. *Org. Biomol. Chem.* **2012**, *10*, 8868–8876.
- (23) Potter, B. V. L.; Connolly, B. A.; Eckstein, F. *Biochemistry* **1983**, *22*, 1369–1377.
- (24) (a) Burgers, P. M. J.; Eckstein, F. *Proc. Natl. Acad. Sci. U. S. A.* **1978**, *75*, 4798–4801. (b) Bryant, F. R.; Benkovic, S. J. *Biochemistry* **1979**, *18*, 2825–2829.
- (25) Borer, P. N. Optical properties of nucleic acids, absorption and circular dichroism spectra. In *Handbook of Biochemistry and Molecular Biology: Nucleic Acids*, 3rd ed.; Fasman, G. D., Ed.; CRC Press: Cleveland, OH, 1975; Vol. 1, pp 589–595.